ICSO 2016

International Conference on Space Optics

Biarritz, France

18–21 October 2016

Edited by Bruno Cugny, Nikos Karafolas and Zoran Sodnik

FOV mask optimization for miniaturized radiometers

F. J. Alvarez-Ríos

J. J. Jiménez

International Conference on Space Optics — ICSO 2016, edited by Bruno Cugny, Nikos Karafolas,
Zoran Sodnik, Proc. of SPIE Vol. 10562, 105625A · © 2016 ESA and CNES
CCC code: 0277-786X/17/$18 · doi: 10.1117/12.2296140

FOV MASK OPTIMIZATION FOR MINIATURIZED RADIOMETERS

F.J Alvarez-Ríos[1], J.J Jimenez[1].
[1]*Instituto Nacional de Técnica Aeroespacial – INTA, Spain*

I. INTRODUCTION

This paper presents the design, characterization and simulation of the field of view (FOV) masks used for the MetSIS, DREAMS SIS and RDS instruments

[1],[2][3],[4]. These instruments are miniaturized solar radiometers based on Schott filters, interference filters and Si-photodiode detector to make spectrally measurements. Due the structural and mechanical restriction and limitation for the opto-mechanical radiometer development, the idea of used standard baffles to limit the FOV was replaced by the use of the presented FOV masks, Fig.1

(a) (b)

Fig.1: a)Distribution of drilled holes b) Optomechanical FOV masks employed for the RDS instruments.

The FOV masks work like an optical baffle allowing the modification of the field of View. Basically, the element is a set of drilled holes, see Fig.1.a, from diameter of 0.5 mm up to 1.5 mm in anodized aluminum structures and thickness from 0.5 mm up to 2 mm. The structures were anodized in black and integrated in the opto-mechanical setup Fig.1.b

The FOV mask has been designed to achieve FOV of 5º and 15º in the case of the RDS instrument, and 38º and 45º in the case of DREAMS-SIS instrument. The experimental FOV measured (angular response) doesn't follow the theoretical equation that mask were designed for. Experimental results have showed discrepancies with theory especially with FOV masks with small FOV (5º-15º). The reason is due the black surfaces like anodized aluminum exhibit different optical reflectance behavior in terms of the angle of incidence. For scattering angles (>80º) respect to the normal incidence on aluminum sample, the reflectivity is increased and the optical behavior is almost specular, that is FOV mask case between 5º and 15º. In order to optimize future FOV masks designs, internal specular reflections have been simulated using ray-trace technique. Moreover, the specular component of the anodized aluminum employed for the mask development has been measured in order to fit the parameters needed to simulate the FOV masks and predict their angular optical response behavior.

I. THEORETICAL DESING

The theoretical FOV of a FOV mask it is calculated according to:

$$\mathrm{FoV} = \mathrm{atan}\left(\frac{D}{L}\right) \tag{1}$$

The parameters taking in account in the equation are described Fig. 2

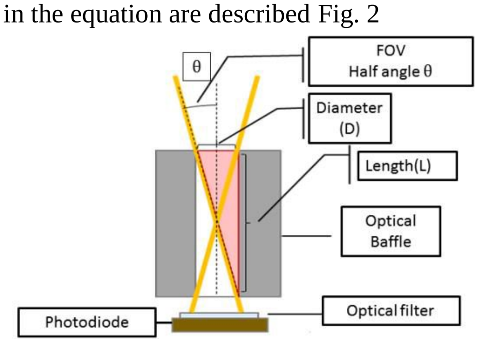

Fig. 2: Hole of FOV masks parameters

II. OPTICAL CHARACTERIZATION

The optical characterization is the measurement of the angular response of the FOV to use it as the merit function, and the specular spectral reflectivity measurement to estimate the fit coefficient parameters for the fitting.

A. ANGULAR RESPONSE FOR THE OPTOMECHANICAL SET-UP

The angular characterization set up employed to perform the angular response of the DREAMS-SIS instrument is described in [9],[10]. It was reused for the characterization of the FOV masks .

(a) (b) (c)

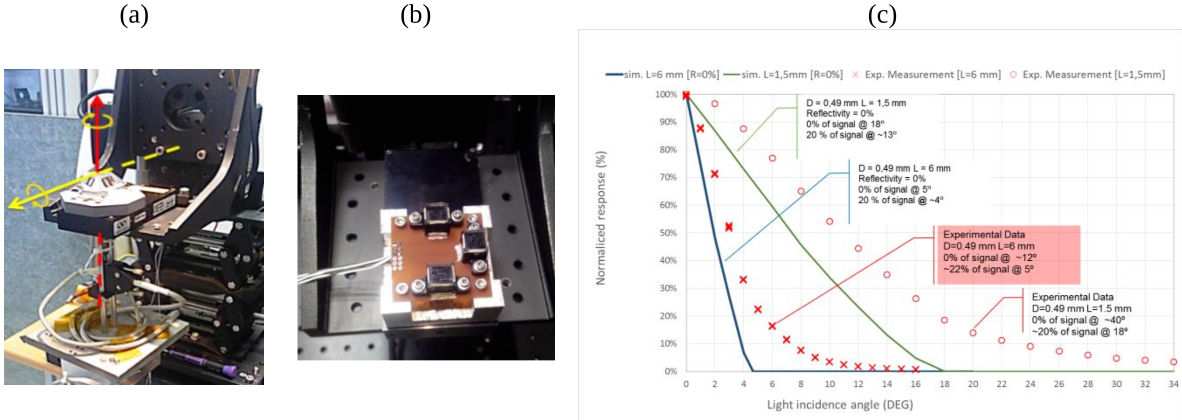

Fig. 3: a) Rotatory optomechanical set-up used during DREAMS-SIS angular calibration b) Set of FOV mask employed during the characterization c) Result and theoretical FOV comparison.

The rotatory stage from Fig. 3a and Fig. 3b provide an automated angular characterization and is controlled by an EGSE software designed to perform angular rotation, sample and stores the detector output. The source used for the calibration was a Xenon Lamp. The sensor are set at a distance large enough (higher than 4.5 meters) from the lamp, from that point of view the source can be considered as a point source emitting spherically. The area of illumination (50x50 cm) covered completely the sensing area (<10x10cm).

The results are shown in Fig. 3c, for the case of a hole diameter of 0.49 mm and two different thickness of 1.5 mm and 6 mm that correspond to the FOV masks design of 5º and 15º respectively. The deviation is significant as can be seen Fig. 3c, for the 5º FOV mask we have a different between theory and experimental of 7º when the angular response has 0% value, and 2º at 20% vale.

In the 15º FOV mask case the difference is higher than 15º for the angular response at 0%. In the case of 20% angular response, the value the difference is 5º.

B. SPECTRAL REFLECTIVITY MEASUREMENTS

The spectral reflectivity measured was the specular reflection in order to verify and estimate it versus the angular incident of light. The set up procedure consisted firstly in measure a reference value with a collimated xenon lamp without the sample with a spectrometer equipped with an optical diffuser head. Then, the sample is introduced rotated with an angle β and the optical head is moved to in one axis direct to measure the light direct reflection.

The calculation of the reflection angle is shown in Fig. 4.a. The spectral measurement of reflected light for 2.9º and 5.2º is shown Fig. 4.b. Finally, the specular mean reflectivity for the VIS (400-700 nm) and NIR (700-1000 nm) is represented in Fig. 4.b.

(a) (b) (c)

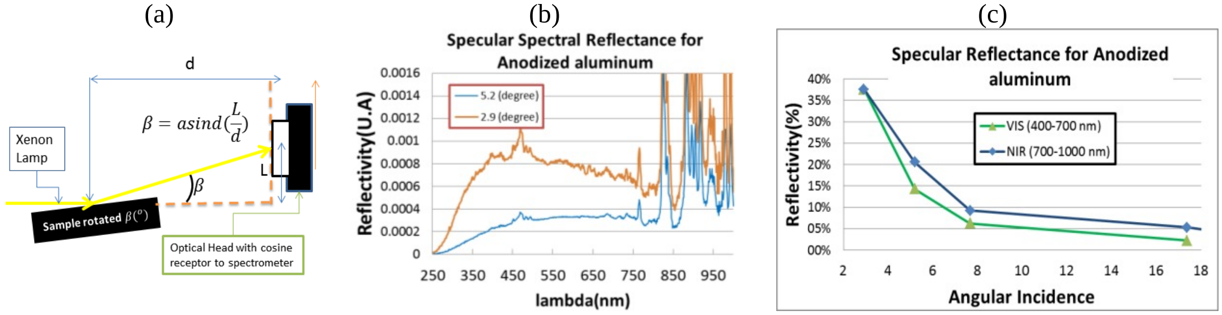

Fig. 4: a) Scheme for angular reflectivity measurement b) Spectral specular reflectance c) Specular reflectance in the VIS and NIR respect to angular of incidence.

III. SIMULATIONS

The simulation has been developed like a tool to predict the optical behavior of future FOV designs made by the same anodized aluminum treatment. It has been used the CAD-Model of the FOV mask with diameter 0.49 mm and 1.5 mm and 6 mm respectively. The simulation consisted on trace rays with different light angle conditions. A source surface has been defined to trace the rays. Then, a macro automatized the process to rotate the source to a specific angle of emission. The material property has been considered specular.

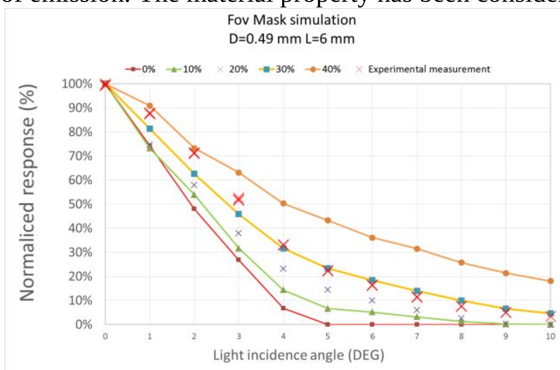

Fig. 5: Simulation for FOV-mask D=0.49 L=6 mm for several reflectivities

The reflectivity in each simulation was modified since 10% up to 40% for each simulation. It can be seen in Fig. 5 the value of the angular response for several reflectivities. It has been chosen 30% value as best fit, because, it matches better in the region that define the maximum angle acceptance. This value is needed to predict future designs based in this material.

Then, in order to short the optical FOV, mask diameter holes were reduced from 0.49 mm to 0.31 mm. To estimate the optical angular behaviour of new designs, a simulation was performed. The simulation results are presented in Fig. 6.

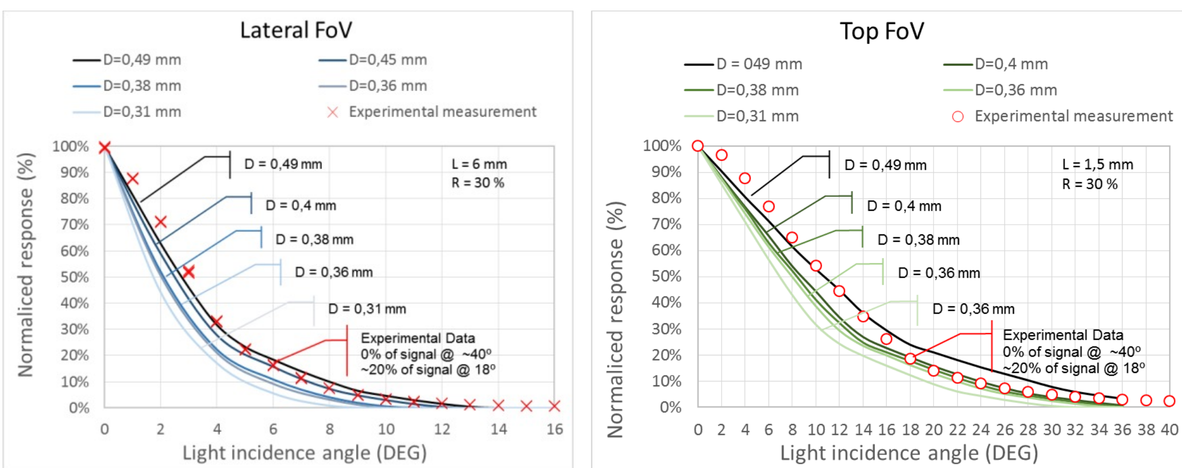

Fig. 6: FOV mask simulations modifying the parameter D a) L=6 mm , 30% reflectivity case c) L=1.5 , 30% reflectivity case.

D. CONCLUSIONS AND FUTURE WORK

A simulation tool has been developed to simulate the angular response for the FOV mask and predict the maximum acceptance angle of the developed designs. The model has feedback from experimental measurements like the angular response of several designs and the measurent of the spectral reflectivity for the specular case.

As future work, new structures are planning to be developed by 3D impression in order to achieve better FOV mask according to the design. Currently, it is under study the use new materials coating to improve the absorption of the surface material employed in the FOV mask development.

E. ACKNOWLEDGMENTS

Part of this work has been funded with the help of the Spanish National Research, Development and Innovation Program, through the grants AYA2011-29967-C05-01 and ESP2014-54256-C4-3-R.

[1] V. Apestigue, J.J. Jiménez et al "2014 DREAMS-SIS: A Miniature Instrument for the Measurement of Atmospheric Optical Depth on ExoMars 2016 EDM". *International Workshop on Instrumentation for Planetary Missions*, Greenblet, Maryland (IPM-2014).

[2] I.Arruego, et al., "DREAMS-SIS, the solar Irradiance Sensor on-board the ExoMars 2016 Lander: concept, design and operating principles", unpublished.

[3] F. Esposito, et al., DREAMS for the ExoMars 2016 mission: a suite of sensors for the characterization of Martian environment, *European Planetary Science Congress*,(2013).

[4] http://exploration.esa.int/mars/48898-edm-science-payload

[5] V. Apéstigue , I. Arruego, et al, Radiation and Dust Sensor for MARS2020: technical design and development status overview" EPSC Abstracts Vol. 10, EPSC2015-813-2, 2015 European Planetary Science Congress 2015

[6] Eric C. Fest. *"Stray Light Analysis and Control"* ISBN 978-0-8194-9325-5 , Published by SPIE, 2013.

[7] "Anodic Coatings for aluminum and aluminum alloys" *Military Standard (MIL-STD),* 8625F (2003)

[8] Remo Tamayo, José Alonso, J.J. Jimenez, Ignacio Arruego, Héctor Guerrero, "*Optical Wireless Links for intra-Satellite Communications: Reflection Models and Hardware Optimization*", AIAA Journal Of Aerospace Computing, Information and Communication, Vol. 7, No. 3, pp:118-133, Iss. 12, 2010.

[9] J. Jimenez, F.J. Alvarez-Ríos, et al., "Calibration OGSE for multichannel radiometer for Mars atmosphere studies". *International conference on space Optics (ICSO).* Biarritz, France (2016).

[10] F.J Alvarez-Ríos, J.J.Jimenez, et al "Determination of the angular response function for miniaturized radiometric instruments: aplication to the DREAMS-SIS instrument", unpublished.